NASA TECHNICAL NOTE

NASA TN D-4389

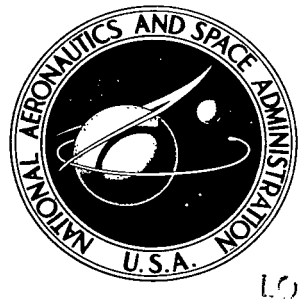

NASA TN D-4389

COLD-AIR INVESTIGATION OF A TURBINE FOR HIGH-TEMPERATURE-ENGINE APPLICATION

III - Overall Stage Performance

by Warren J. Whitney, Edward M. Szanca, Bernard Bider, and Daniel E. Monroe

Lewis Research Center
Cleveland, Ohio

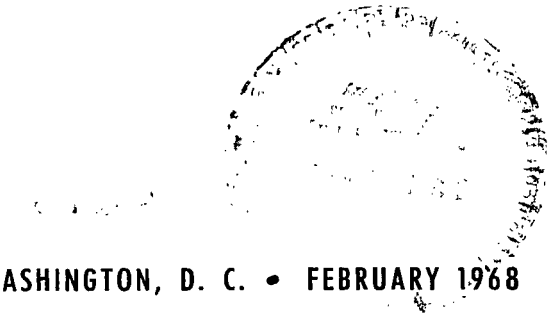

NATIONAL AERONAUTICS AND SPACE ADMINISTRATION • WASHINGTON, D. C. • FEBRUARY 1968

COLD-AIR INVESTIGATION OF A TURBINE FOR HIGH-TEMPERATURE-ENGINE APPLICATION

III - Overall Stage Performance

By Warren J. Whitney, Edward M. Szanca,
Bernard Bider, and Daniel E. Monroe

Lewis Research Center
Cleveland, Ohio

NATIONAL AERONAUTICS AND SPACE ADMINISTRATION

For sale by the Clearinghouse for Federal Scientific and Technical Information
Springfield, Virginia 22151 – CFSTI price $3.00

COLD-AIR INVESTIGATION OF A TURBINE FOR HIGH-TEMPERATURE-ENGINE APPLICATION III - OVERALL STAGE PERFORMANCE

by Warren J. Whitney, Edward M. Szanca, Bernard Bider, and Daniel E. Monroe

Lewis Research Center

SUMMARY

An experimental investigation was made to determine the performance of a 30-inch (0.762-m) single-stage turbine which was designed to incorporate the physical features associated with turbines for high-engine-temperature application. The characterizing features for this application, which are pertinent to the turbine aerodynamic performance, are thick blade profiles, blunt leading and trailing edges, and low solidity.

The turbine developed equivalent design specific work output at equivalent design speed with an efficiency of 0.923 which was the highest efficiency obtained over the range of conditions investigated. The corresponding equivalent mass flow, 40.64 pounds per second (18.434 kg/sec), is 1.8 percent greater than the design mass flow. In view of the efficiency that was obtained with the turbine it was concluded that the compromising of the airfoil shapes, which was necessary because of cooling considerations, did not noticeably impair the turbine performance.

The design mean radius velocity diagram is compared with that calculated from the experimental results obtained at equivalent design speed and equivalent design specific work output. The comparison indicated that an overexpansion occurred across the stator and that the reaction across the rotor was reduced. This effect was attributed to an excessive passage area allowance at the rotor outlet which resulted from the assumed design efficiency being lower than the experimentally obtained efficiency.

INTRODUCTION

Some advanced aircraft engines require increased cycle temperatures to achieve their performance goals. The turbines for these engines can be characterized by thick blade forms, blunt leading and trailing edges, and low solidity. The thick blunt blade forms are required to incorporate internal coolant passages and the low solidity to minimize the amount of blade surface area. These blade forms are, therefore, compromised from what would be considered optimum from an aerodynamic standpoint.

A 30-inch cold-air research turbine was designed with physical characteristics that were selected to typify those of a turbine for high-temperature application. The turbine design procedure and the overall stator investigation are presented in reference 1. The results obtained in the reference showed that the stator passed design equivalent mass flow at design pressure ratio. The stator also produced very close to design flow angle over the range of outlet critical velocity ratio investigated. The results of detailed surveys made immediately downstream of the stator blade trailing edge are presented in reference 2. The total pressure contours did not indicate any prominent secondary flow loss cores, and the overall kinetic energy loss was only slightly larger than that of a high solidity blade with a thin profile. Thus, it was concluded that the stator component performed well even though the blading profiles were somewhat compromised.

This report presents the results obtained in the experimental investigation of the complete turbine stage. The rotor assembly was installed in the test facility and the turbine was operated over a range of speeds and pressure ratios. Turbine inlet conditions were 30 inches of mercury absolute (1.0159×10^5 N/m^2) and about 80° F (299.8° K). The turbine was investigated over a range of equivalent speeds from 40 to 100 percent design speed and over a range of total pressure ratio from 1.4 to 2.0. Turbine efficiency based on total pressure ratio was used to indicate the turbine performance.

SYMBOLS

A area, ft^2 (m^2)

c blade chord, ft (m)

g force-mass conversion constant, 32.174 ft/sec^2

h specific enthalpy Btu/lb (J/kg)

l blade length, ft (m)

N rotational speed, rpm (rad/sec)

p absolute pressure, lb/ft^2 (N/m^2)

R gas constant, 53.34 ft-lb/(lb)(^oR) (287 J/(kg)(^oK))

r radius, ft (m)

s blade pitch, ft (m)

T temperature, ^oR (^oK)

U blade velocity, ft/sec (m/sec)

V absolute gas velocity, ft/sec (m/sec)

W gas velocity relative to rotor blade, ft/sec (m/sec)

w mass flow rate, lb/sec (kg/sec)

α absolute gas flow angle measured from axial direction, deg

α_r average absolute gas flow angle measured from axial direction at rotor outlet used in eq. (2), deg

β relative gas flow angle measured from axial direction, deg

γ ratio of specific heats

δ ratio of inlet pressure to U.S. standard sea-level pressure

η efficiency based on total pressure ratio

θ_{cr} squared ratio of critical velocity at turbine inlet to critical velocity of U.S. standard sea-level air

τ torque, ft-lb (N-m)

Subscripts:

cr condition at Mach 1

m turbine mean section

t turbine tip section

u tangential component

x axial component

0 station at turbine inlet (see fig. 4)

1 station at stator outlet

2 station at rotor outlet

Superscript:

' total state

APPARATUS, INSTRUMENTATION, AND PROCEDURE

As indicated in the INTRODUCTION, the turbine that was a single-stage cold-air research turbine that had a 30-inch (0.762-m) tip diameter and was designed with the physical features characteristic of a turbine for high-temperature-engine application. The geometric characteristics of the blading are listed in table I.

The design procedure used to evolve the blade shapes was discussed in reference 1. A sketch showing the blade passages and profiles is shown in figure 1 and the blading coordinates are listed in table II. The design requirements of the turbine are summarized as follows:

Equivalent specific work output, h/θ_{cr}, Btu/lb (J/kg)	17.00 (39 570)
Equivalent mean blade speed, $U_m/\sqrt{\theta_{cr}}$, ft/sec (m/sec)	500 (152.4)
Equivalent mass flow, $w\sqrt{\theta_{cr}}/\delta$, lb/sec (kg/sec)	39.9 (18.098)

As mentioned in reference 1 the efficiency used in the design procedure to size the rotor outlet area was 0.885, which was selected using reference 3. Applying the efficiency-size correlation of reference 4 results in an efficiency of 0.913 being predicted for this turbine design. However, the use of the lower efficiency estimation was felt to be more conservative in this instance, considering that the subject blading might incur larger profile losses than those generally used in performance estimation procedures. Furthermore, using a given efficiency in the design procedure does not preclude obtaining a higher efficiency experimentally.

The design velocity diagram that was developed to meet the design requirements was shown in reference 1 and is included herein for convenience in figure 2. The turbine stator assembly was the same as that used in references 1 and 2. The rotor assembly consisted of 61 blades that were machined from aluminum alloy bar stock. After the rotor was assembled, the blade tips were machined to provide a radial clearance of 0.030 inches (0.0762 cm). This clearance results in a clearance to passage height ratio of 0.0075, and the tip clearance loss for this turbine would be quite small. A photograph of the turbine rotor assembly is shown in figure 3.

The test facility (fig. 4) was the same as described in reference 1 except for the inclusion of the turbine rotor assembly and the absorption dynamometer. A diagrammatic

sketch of the turbine test section is shown in figure 5. The turbine was operated with dry pressurized air from the combustion air system. A calibrated Dall tube, which was located in a straight run of the air supply piping, was used to meter the mass flow. Turbine inlet and outlet pressures were set using butterfly throttle valves. The flow at the turbine outlet was throttled to the altitude exhaust system. The turbine power output was absorbed with a water cooled eddy current dynamometer.

The Dall tube instrumentation required for the mass flow measurement consisted of the air stream temperature, the upstream pressure, and the throat pressure. The upstream pressure was read on a mercury fluid manometer and the differential between upstream and throat pressures was read on a tetrabromoethane fluid manometer. The air temperature at the Dall tube was measured with a thermocouple and read with a direct reading self-balancing potentiometer.

At the turbine inlet (sta. 0, fig. 5) the instrumentation consisted of static pressure, total temperature, and total pressure. The temperature was measured with two thermocouple rakes, each containing five thermocouples, that were located at the area center radii of five equal annular areas. Static pressure was obtained from eight taps with four on the inner wall and four on the outer wall. The inner and outer taps were located directly opposite each other and were spaced 90° apart about the circumference. Total pressure was measured with four total pressure probes spaced 90° apart circumferentially on the area center radius.

The instrumentation at station 1, between the stator and the rotor, was comprised of eight static pressure taps. These taps were spaced 90° apart with four on the inner wall and four on the outer wall as described for station 0.

At the turbine outlet, station 2, the instrumentation included static pressure and flow angle. The static pressure was measured with eight wall taps located as described for stations 0 and 1. The outlet flow angle was measured with five angle sensitive probes and self-alining probe actuators spaced at approximately equal circumferential intervals. The outlet flow angle measurements were made at five radial positions corresponding to the area center radii of five equal annular areas.

The turbine rotative speed was measured with an electronic counter in conjunction with a magnetic pickup and a sprocket located on the turbine shaft. The turbine torque was measured on the dynamometer stator with a strain-gage-type load cell. The load cell and digital voltmeter readout were calibrated at the start of each day's running.

All of the pressures at the turbine test section were obtained by photographing a mercury filled manometer board. The temperatures were read in the control room on a direct reading self-balancing potentiometer.

Turbine performance was based on total pressure ratio. The inlet total pressure was calculated (as in ref. 1) from the static pressure, mass flow, annulus area, and total temperature using the following equation:

$$\frac{p'_0}{p_0} = \left[\frac{1}{2} + \sqrt{\frac{1}{4} + \frac{\gamma - 1}{2g\gamma}\left(\frac{w}{p_0 A}\right)^2 RT'_0}\right]^{\gamma/(\gamma-1)} \tag{1}$$

The outlet total pressure was also calculated using static pressure, mass flow, average flow angle, annulus area, and total temperature:

$$\frac{p'_2}{p_2} = \left[\frac{1}{2} + \sqrt{\frac{1}{4} + \frac{\gamma - 1}{2g\gamma}\left(\frac{w}{p_2 A}\right)^2 \frac{RT'_2}{\cos^2 \alpha_r}}\right]^{\gamma/(\gamma-1)} \tag{2}$$

The temperature T'_2 used in equation (2) was derived from the inlet temperature, torque, mass flow, and speed. The flow angle α_r used in this equation must be taken as the average divergence from the axial direction, irrespective of sign.

The performance data was used to construct the performance map in the following manner. The observed data points were plotted in the form of equivalent mass flow $w\sqrt{\theta_{cr}}/\delta$ and equivalent torque τ/δ, each as a function of total to static pressure ratio p'_0/p_2. On these plots smooth lines were faired for each speed. Then the total pressure ratio p'_0/p'_2, equivalent specific work output $\Delta h/\theta_{cr}$, and efficiency η were computed for each data point using the faired values of weight flow and torque.

RESULTS AND DISCUSSION

The experimental results include the overall turbine performance, mass flow characteristics, variation of turbine outlet flow angle, static pressure distribution, and a comparison of the experimentally obtained mean radius velocity diagram with the design diagram. These items will be discussed in this order in the following sections.

Overall Performance

The basic data obtained from the turbine tests are shown in figures 6 and 7 with equivalent torque τ/δ and equivalent mass flow $w\sqrt{\theta_{cr}}/\delta$ shown as a function of the total to static pressure ratio p'_0/p_2. The curves on the two figures were faired for each value of percent of equivalent design speed investigated. The performance map (fig. 8) was then constructed from crossplots, computed from the faired values of figures 6 and 7. The overall performance (fig. 8) is represented by curves of equivalent specific

enthalpy drop $\Delta h/\theta_{cr}$ as a function of mass flow-speed parameter wN/δ for the various equivalent speeds, with constant total pressure ratio lines and efficiency contours superimposed. The turbine attained generally high efficiencies with the efficiency varying from 0.70 to 0.92 for the range of conditions investigated. At the condition of design work output, $\Delta h/\theta_{cr}$ = 17.00 Btu per pound (39 573 J/kg) and at design equivalent speed, the efficiency is seen to be somewhat in excess of 0.92. From the design speed crossplot of $\Delta h/\theta_{cr}$ as a function of p'_0/p'_2, equivalent design specific work output occurred at a pressure ratio of 1.751 which corresponds to an efficiency value of 0.923.

The total efficiency obtained from the experimental results (0.923) is considerably higher than that used in the design (0.885). As mentioned previously, this design efficiency was used principally to obtain the rotor exit state conditions and was selected based on curves presented in reference 3. Such curves were considered in the reference as representing reasonable levels of efficiency for given turbine work and speed requirements. Also, as discussed previously, a subsequent study of single-stage turbine performance was made in reference 4 using the basic equations of reference 3 but with specific consideration of size effects. Using the loss parameter as obtained in reference 4 to reflect the size of the subject turbine (stator throat area was used for correlation), a total efficiency of 0.913 was computed. Thus, from these considerations, the major difference between experimental and design efficiency appears to be due to the test turbine being large in size. In addition, other factors contributing to the higher efficiency would include (1) the type of velocity diagram used with some exit whirl used in the subject design as compared with zero whirl used in the curves of reference 3 and (2) the running clearance of the subject turbine being very small.

It was also considered of interest to compare the design point performance of the subject turbine with that predicted by other reference procedures. Applying the method of reference 5, which considers the various losses within the turbine to a greater detail than that of reference 3, a total efficiency of 0.929 was predicted. From figure 3.37 of reference 6 (a rather general emperical correlation of efficiency as a function of velocity diagram parameters), an efficiency of 0.928 (based on zero tip loss) is indicated.

From these considerations, it appears that the total efficiency of 0.923, obtained for the subject turbine, is consistent with that expected for a unit of similar design velocity diagrams, size, and running clearance. As such, it can then be concluded that the compromising of the airfoil shapes from cooling considerations did not impair the turbine performance to any marked degree.

Mass Flow Characteristics

The equivalent mass flow passed by the turbine is shown in figure 9 as a function of

total pressure ratio. The separation of the various speed lines in figure 9 indicates that the flow is being controlled by the rotor component. At 40 percent of equivalent design speed the rotor choked at a total pressure ratio of about 1.65 and at 100 percent design speed the choking pressure ratio is approximately 2.0. At design equivalent speed and at the pressure ratio (1.751) corresponding to equivalent design specific work output the equivalent mass flow was 40.64 pounds per second (18.434 kg/sec). This value represents a flow 1.8 percent greater than the design value. The results of reference 1 showed that the stator component passed design flow at the design total-to-static pressure ratio. Thus the subject results would indicate that, with the turbine operating at equivalent design speed and equivalent design specific work output, the total-to-static pressure ratio across the stator must have been greater than design. This excess mass flow would then indicate that the passage area provided in the rotor was more than necessary. This reasoning is consistent with the efficiency that was obtained. In the design procedure, an efficiency of 0.885 was assumed and this efficiency value was used to determine the rotor outlet total pressure and the rotor outlet flow area. If the experimentally obtained efficiency of 0.923 had been used in the design procedure, a higher outlet total pressure and static pressure would have resulted and the required rotor outlet area estimated in the design procedure would have been smaller.

Rotor Outlet Flow Angle

The flow angle at the turbine outlet is shown in figure 10 as a function of total pressure ratio. The angle shown is the numerical average of the five angle measurements mentioned in the section APPARATUS, INSTRUMENTATION, AND PROCEDURE. The negative sign of the angle corresponds to a positive contribution to the work output. Although a certain amount of scatter is present, there is a reasonably distinct variation of flow angle with pressure ratio at each rotor speed. The average angle indicated at the conditions of equivalent design specific work output at equivalent design speed is -15.2°. This angle can be compared with the value of -17.95° which is an average flow angle based on the hub, mean, and tip values of the design velocity diagram. This angle variation from that of the design velocity diagram is also consistent with the premise that the flow overexpanded in the stator. Thus design work was developed with a smaller contribution of rotor outlet whirl velocity.

Static Pressure Distribution Through Turbine

The design static pressures at the hub and tip sections were obtained for the instru-

mented stations from the design velocity diagram and the loss assumptions that were used in the design procedure. This static pressure distribution is shown in figure 11 with all pressures ratioed to inlet total pressure. Also shown in the figure is the experimental static pressure distribution that was obtained at equivalent design speed and equivalent design specific work output. A comparison of the design and experimental pressure variations through the turbine shows that the flow overexpanded in the stator. This would be expected since it was previously noted that the experimental weight flow at this condition was slightly greater than design. The comparison of pressure levels also shows that the rotor operated with less than design reaction at both hub and tip sections.

Velocity Diagram at the Mean Radius

A mean radius velocity diagram was calculated using the experimentally obtained values of mass flow, specific work output, and average outlet flow angle for the condition of equivalent design specific work output at equivalent design speed. In this procedure the assumption is made that the specific work output, specific mass flow, and flow angle at the mean radius can be taken as the average for the blade row. The rotor outlet velocity was determined from the mass flow, average flow angle, and known total state conditions. The stator outlet velocity was then determined from mass flow and known whirl velocity. The diagram is compared with the design velocity diagram in figure 12. This comparison also shows that a small overexpansion in the stator and a reduced reaction in the rotor were obtained experimentally. The figure also shows that these differences did not affect the flow angles appreciably. Although the mass flow and the pressure drop through the blade rows varied slightly from design this would not be expected to cause any noticeable incidence losses.

SUMMARY OF RESULTS

A 30-inch (0.762-m) single-stage turbine, which was designed to exemplify the aerodynamic problems associated with turbines for high-temperature-engine application, has been investigated experimentally. The experimental results include the efficiency and mass flow characteristics, as well as comparison of the design mean radius velocity diagram with the velocity diagram calculated from the experimental results obtained for the conditions of equivalent design specific work output and equivalent design speed. The pertinent results are summarized as follows:

1. The turbine efficiency obtained at equivalent design speed and equivalent design specific work output was 0.923. From this result, it was concluded that the compromising of the airfoil shapes did not noticeably impair the turbine efficiency.

2. The equivalent mass flow at equivalent design speed and equivalent specific design work output was 40.64 pounds per second (18.434 kg/sec) which represents a value 1.8 percent greater than the design mass flow.

3. A comparison of the design mean radius velocity diagram with that calculated from experimental results obtained at equivalent design speed and equivalent design specific work output indicated there was overexpansion in the stator and reduced reaction in the rotor. This effect was attributed to an excessive passage area allowance at the rotor outlet, which resulted from the assumed design efficiency being lower than the experimental efficiency.

Lewis Research Center,
National Aeronautics and Space Administration,
Cleveland, Ohio, October 26, 1967,
720-03-01-35-22.

REFERENCES

1. Whitney, Warren J.; Szanca, Edward M.; Moffitt, Thomas P.; and Monroe, Daniel E.: Cold-Air Investigation of a Turbine for High-Temperature-Engine Application. I. Turbine Design and Overall Stator Performance. NASA TN D-3751, 1967.

2. Prust, Herman W., Jr.; Schum, Harold J.; and Behning, Frank P.: Cold-Air Investigation of a Turbine for High-Temperature-Engine Application. II. Detailed Analytical and Experimental Investigation of Stator Performance. NASA Technical Note; estimated publication date, January 1968.

3. Stewart, W. L.: A Study of Axial-Flow Turbine Efficiency Characteristics in Terms of Velocity Diagram Parameters. Paper No. 61-WA-37, ASME, 1961.

4. Holeski, D. E.; and Stewart, W. L.: Study of NASA and NACA Single-Stage Axial Flow Turbine Performance as Related to Reynolds Number and Geometry. J. Eng. Power, vol. 86, no. 3, July 1964, pp. 296-298.

5. Ainley, D. G.; and Mathieson, G. C. R.: A Method of Performance Estimation for Axial-Flow Turbines. Rep. No. R and M 2974, Aeronautical Research Council, Great Britain, 1957.

6. Horlock, J. H.: Axial Flow Turbines. Butterworth, Inc., 1966.

TABLE I. - BLADE GEOMETRIC CHARACTERISTICS

Geometric characteristic	Rotor blade	Stator blade
Leading-edge-radius to chord ratio	0.065	0.066
Trailing-edge-radius to chord ratio	0.015	0.015
Maximum thickness to chord ratio	0.20	0.22
Blade chord dimension:		
in.	2.290	2.263
cm	5.82	5.18
Solidity, c/s	1.71	1.385
Aspect ratio, l/c	1.75	1.77

TABLE II. - TURBINE BLADE COORDINATES[a]

(a) Stator

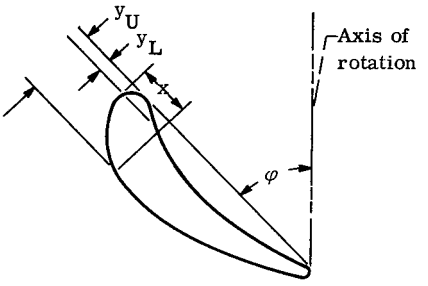

x, in.	Hub		Mean		Tip	
	Orientation angle, φ, deg					
	42.42		41.03		39.67	
	Radius ratio, r/r_t					
	0.7333		0.8666		1.000	
	y_L, in.	y_U, in.	y_L, in.	y_U, in.	y_L, in.	y_U, in.
0	0.150	0.150	0.150	0.150	0.150	0.150
.100	-----	.375	-----	.394	-----	.427
.200	-----	.486	-----	.514	-----	.550
.300	.060	.558	.061	.588	.063	.621
.400	.105	.603	.106	.636	.111	.665
.500	.143	.630	.145	.665	.148	.688
.600	.174	.643	.174	.676	.179	.696
.700	.197	.643	.196	.675	.203	.690
.800	.214	.635	.210	.663	.217	.675
.900	.226	.618	.219	.644	.227	.651
1.000	.230	.595	.223	.619	.231	.625
1.100	.228	.570	.221	.590	.229	.597
1.200	.223	.541	.215	.560	.223	.565
1.300	.212	.508	.205	.527	.214	.535
1.400	.196	.473	.191	.492	.200	.500
1.500	.175	.433	.175	.452	.183	.462
1.600	.153	.391	.155	.410	.163	.422
1.700	.128	.345	.133	.365	.140	.380
1.800	.103	.295	.111	.319	.117	.335
1.900	.075	.242	.086	.267	.095	.287
2.000	.046	.183	.060	.214	.070	.237
2.100	.016	.121	.033	.157	.045	.185
2.197	.035	.035	-----	-----	-----	-----
2.200	-----	-----	.005	.096	.021	.130
2.263	-----	-----	.035	.035	-----	-----
2.327	-----	-----	-----	-----	.035	.035

[a]From ref. 1.

TABLE II. - Concluded. TURBINE BLADE COORDINATES[a]

(b) Rotor

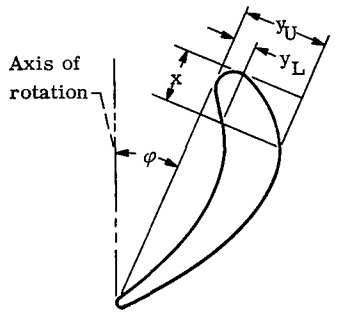

x, in.	Hub		Mean		Tip	
	Orientation angle, φ, deg					
	11.31		22.87		34.67	
	Radius ratio, r/r_t					
	0.7333		0.8666		1.000	
	y_L, in.	y_U, in.	y_L, in.	y_U, in.	y_L, in.	y_U, in.
0	0.150	0.150	0.150	0.150	0.150	0.150
.100	-----	.393	-----	.358	-----	.312
.200	-----	.536	-----	.490	-----	.397
.300	.075	.642	.078	.593	.066	.468
.400	.149	.725	.153	.668	.122	.523
.500	.219	.788	.217	.722	.168	.565
.600	.283	.839	.267	.755	.204	.593
.700	.338	.875	.307	.774	.232	.610
.800	.383	.900	.339	.781	.250	.614
.900	.416	.913	.360	.775	.262	.609
1.000	.439	.913	.373	.759	.264	.594
1.100	.453	.902	.377	.734	.261	.573
1.200	.458	.878	.373	.702	.252	.547
1.300	.454	.845	.362	.664	.237	.519
1.400	.442	.801	.342	.620	.220	.487
1.500	.422	.748	.315	.573	.200	.453
1.600	.393	.689	.283	.523	.177	.416
1.700	.356	.624	.244	.466	.153	.377
1.800	.312	.555	.203	.407	.128	.333
1.900	.260	.481	.159	.346	.103	.288
2.000	.202	.400	.113	.277	.077	.238
2.100	.140	.312	.067	.204	.050	.185
2.200	.072	.216	.022	.125	.022	.128
2.290	-----	-----	.035	.035	-----	-----
2.300	-----	.110	-----	-----	-----	-----
2.321	-----	-----	-----	-----	.035	.035
2.354	.035	.035	-----	-----	-----	-----
	Stacking axis coordinates					
	x = 1.200	y = 0.401	x = 1.110	y = 0.376	x = 1.080	y = 0.337

[a]From ref. 1.

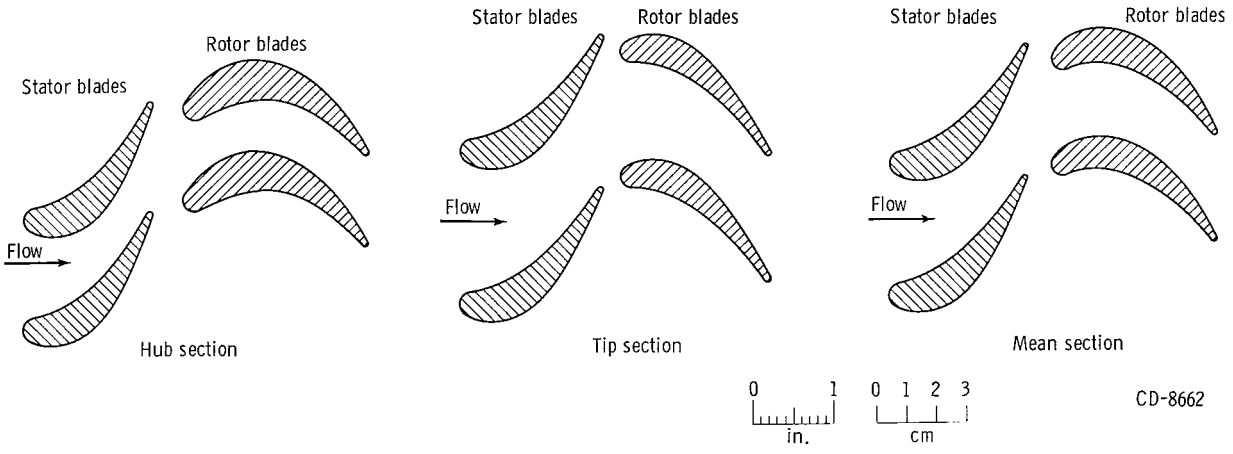

Figure 1. - Sketch of stator and rotor blade profiles and flow passages.

	Hub	Mean	Tip
		ft/sec	
U	423.1	500.0	576.9
$V_{u,1}$	859.8	727.6	630.5
$V_{u,2}$	146.1	123.6	107.2
$V_{x,1}$	308.8	308.8	308.8
$V_{x,2}$	385.8	385.8	385.8
V_1	913.6	790.4	702.1
V_2	412.5	405.1	400.4
W_1	534.9	383.6	313.4
W_2	687.6	733.3	785.4

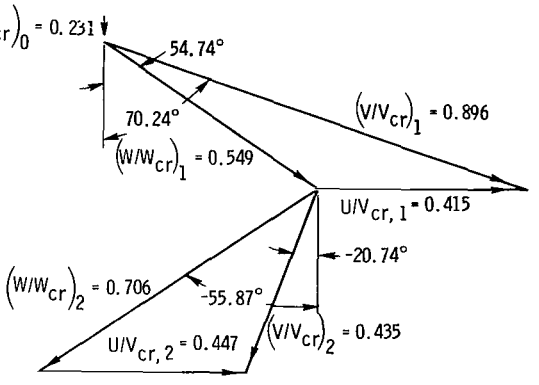

(a) Hub section; radius ratio, r/r_t, 0.733.

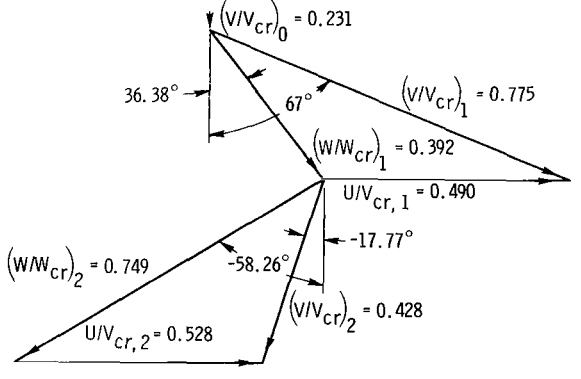

(b) Mean section; radius ratio, r/r_t, 0.8666.

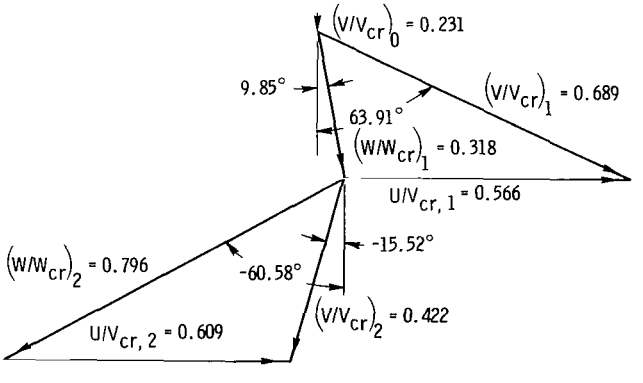

(c) Tip section; radius ratio, r/r_t, 1.000.

Figure 2. - Turbine design velocity diagram. All vector values in table refer to conditions at U. S. standard sea-level air. (From ref. 1.)

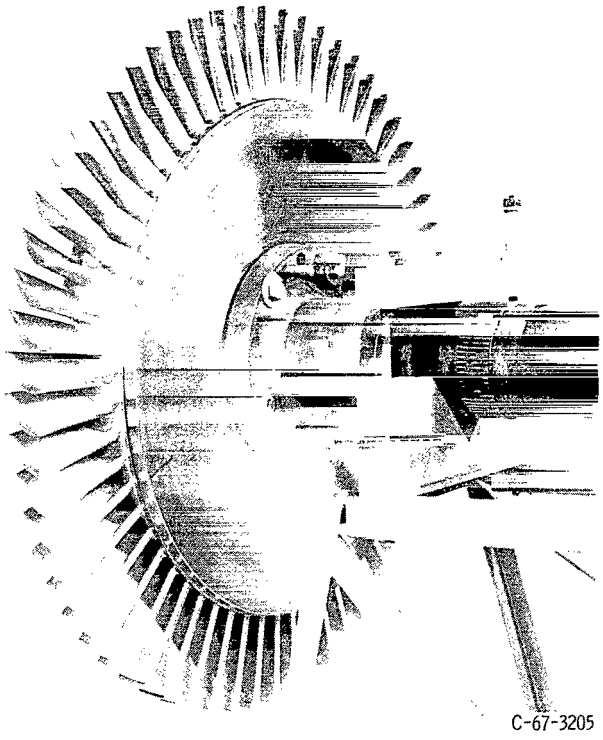

Figure 3. - Photograph of turbine rotor assembly.

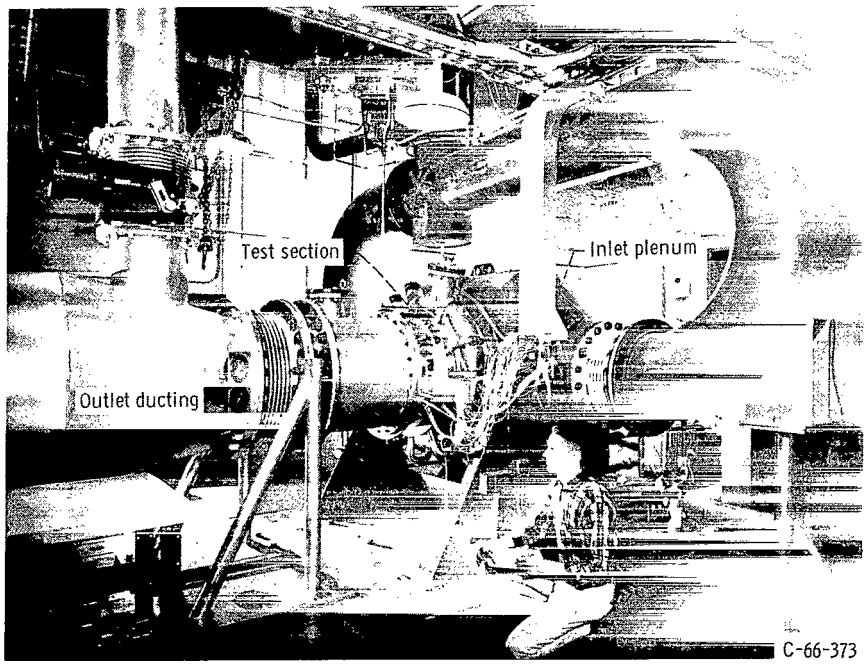

Figure 4. - Test facility.

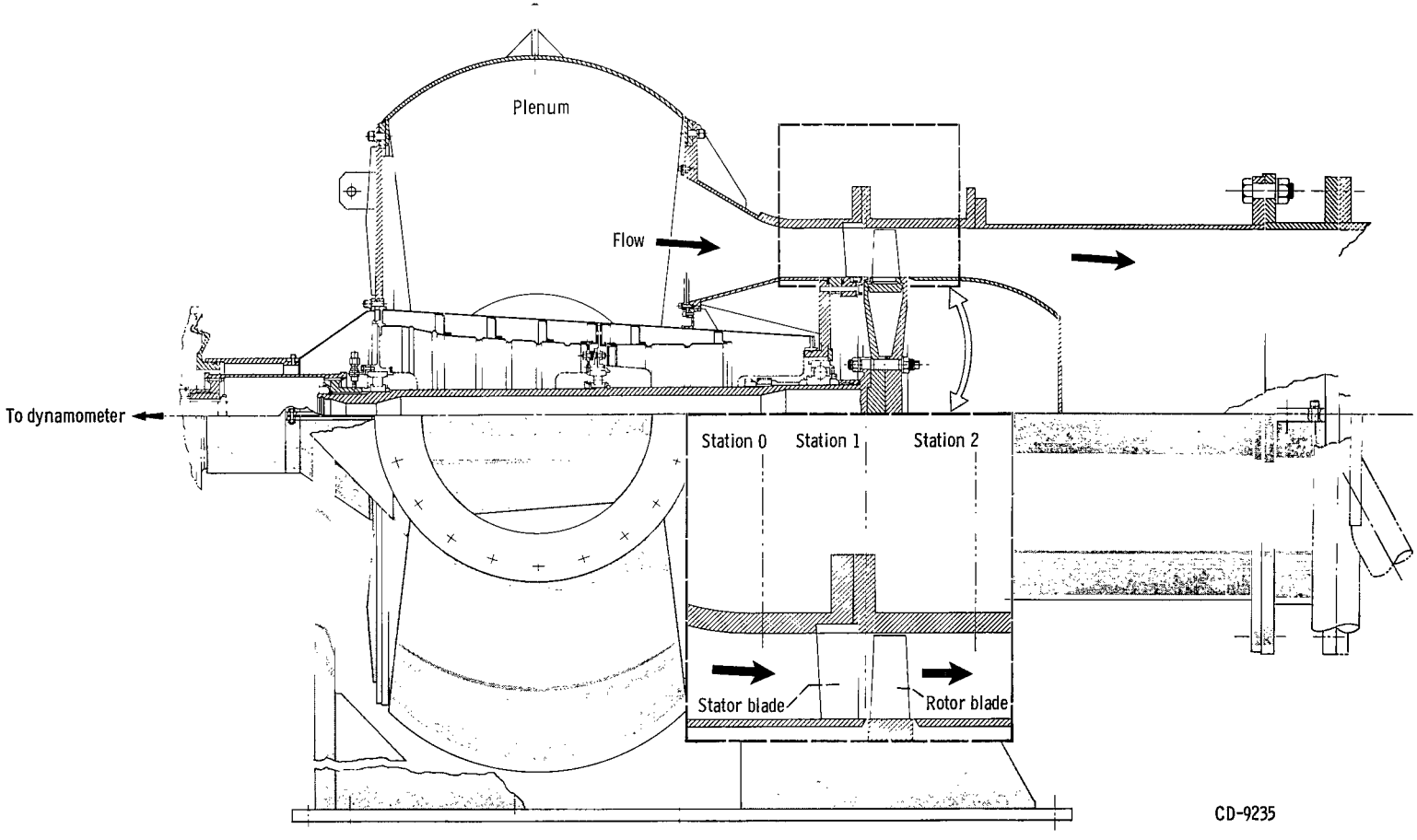

Figure 5. - Schematic diagram of turbine test section.

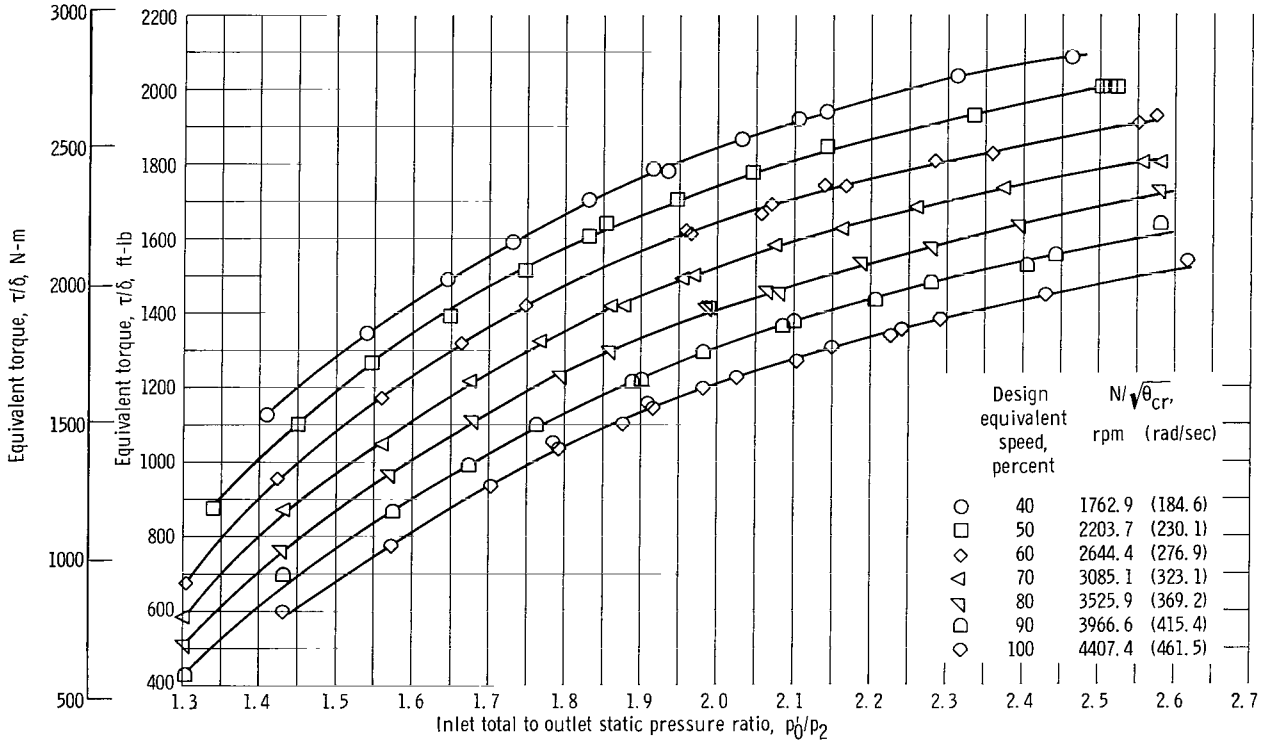

Figure 6. - Variation of equivalent torque with total-to-static pressure ratio for various speeds.

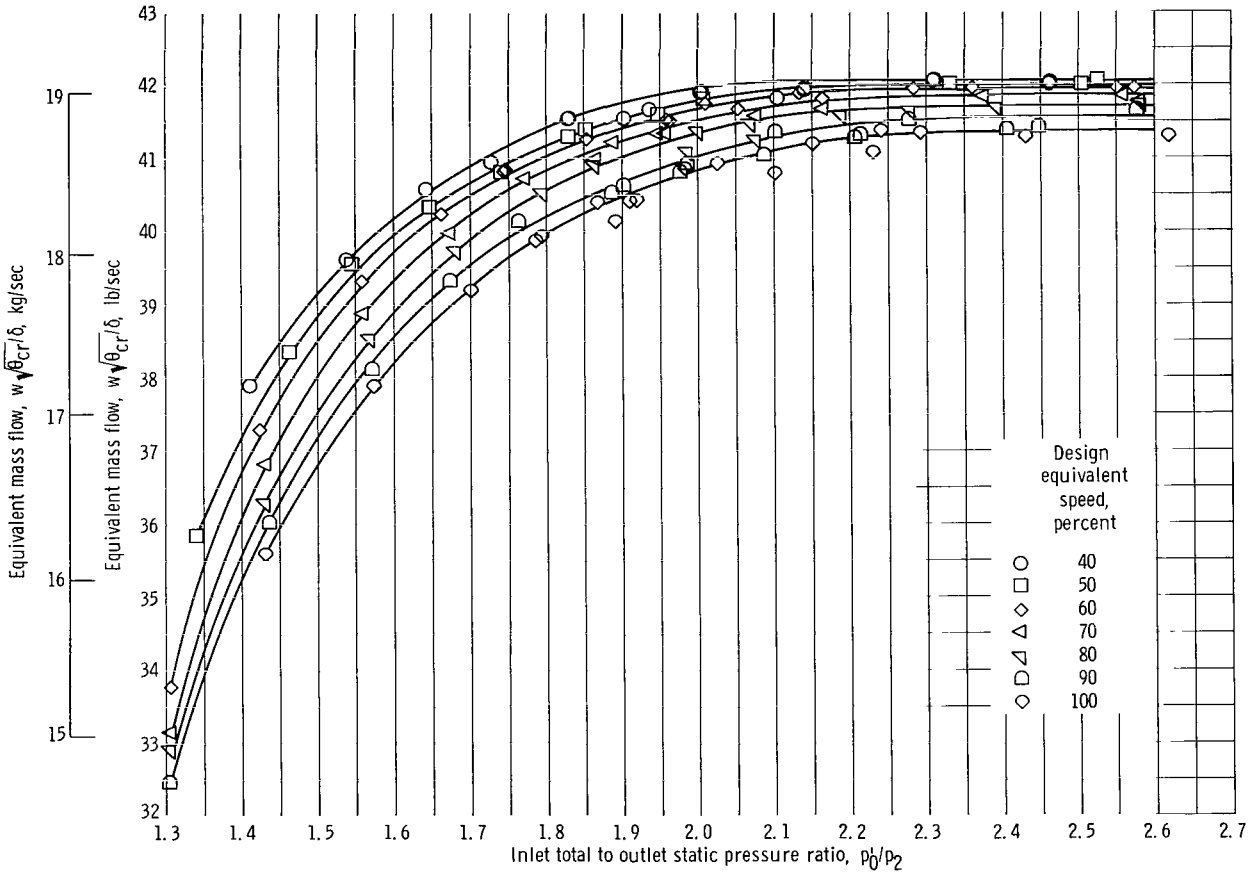

Figure 7. - Variation of equivalent mass flow with total-to-static pressure ratio for various speeds.

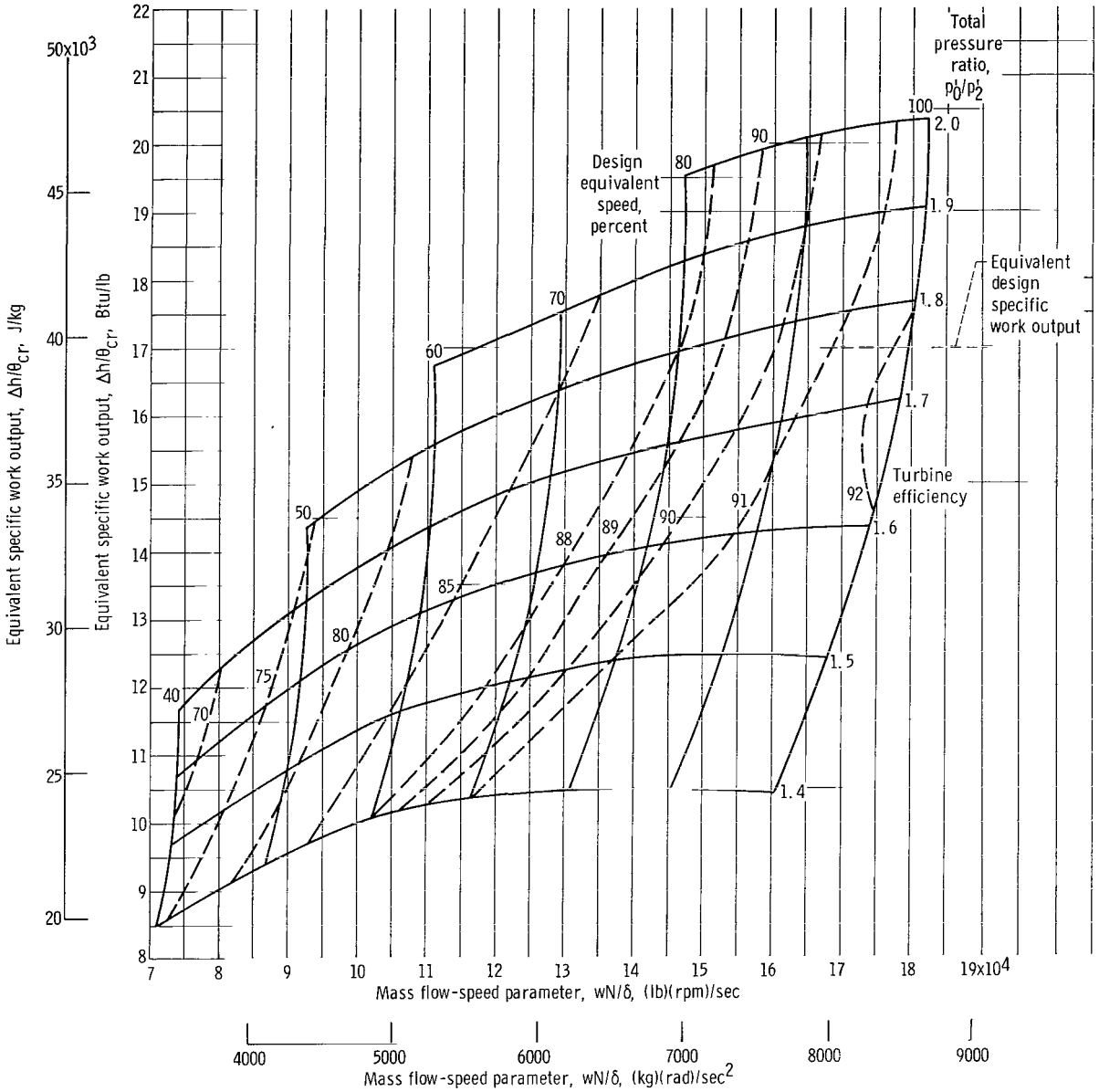

Figure 8. - Overall turbine performance based on total pressure ratio.

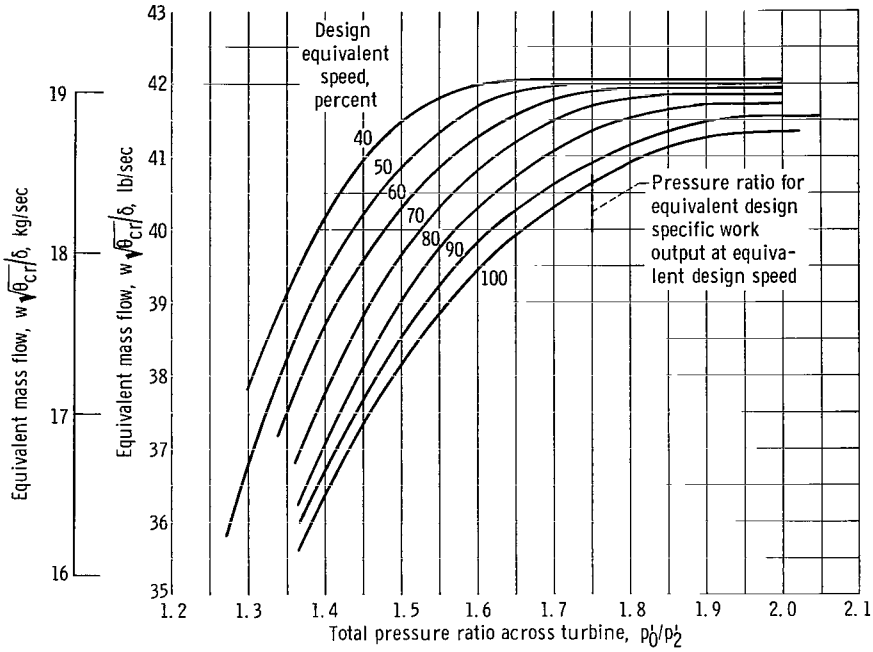

Figure 9. - Variation of equivalent mass flow with total pressure ratio for various speeds.

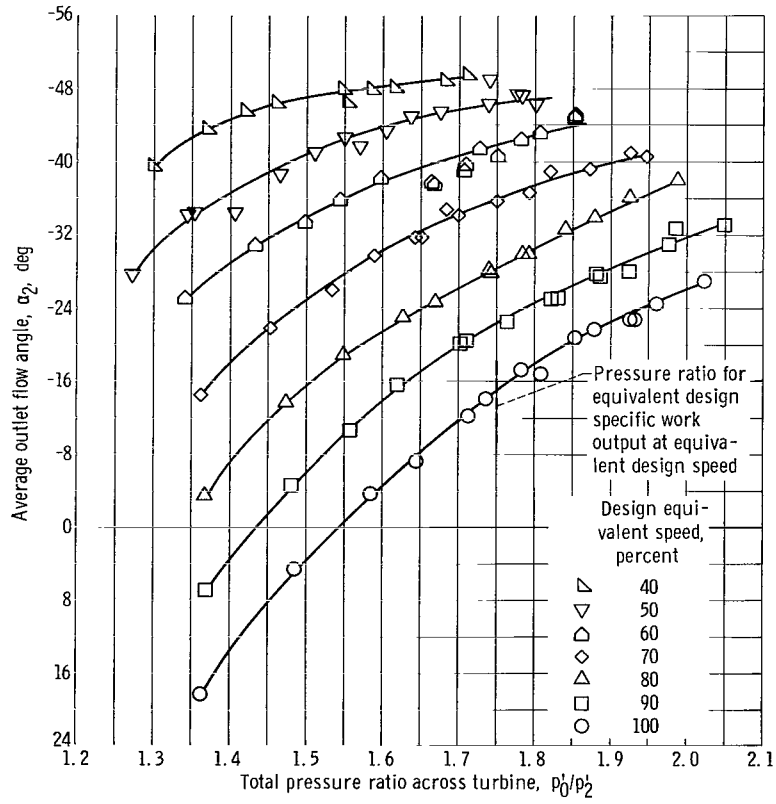

Figure 10. - Variation of outlet flow angle with total pressure ratio for various speeds.

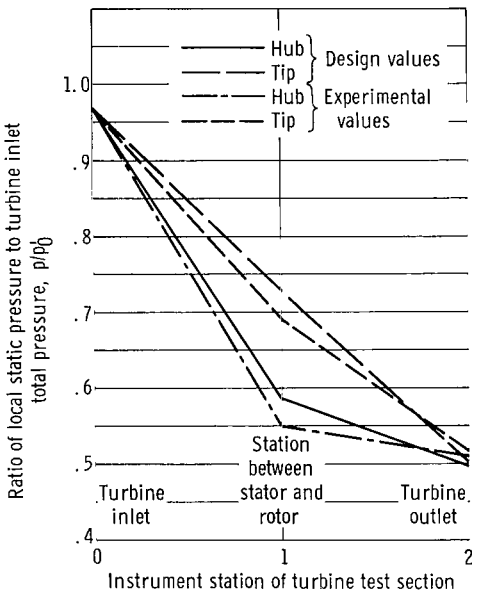

Figure 11. - Comparison of static pressure variation through turbine on inner and outer walls with design static pressure variation. Experimental values correspond to equivalent design specific work output at equivalent design speed and $p'_0/p'_3 = 1.751$.

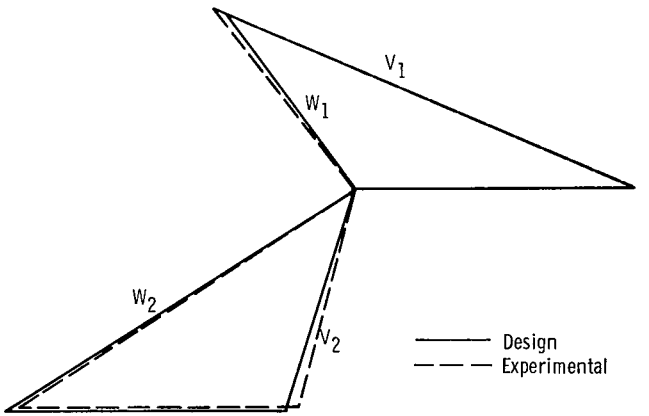

	Design value		Experimental value	
	Velocity			
	ft/sec	m/sec	ft/sec	m/sec
$V_{u,1}$	727.6	221.8	747.6	227.9
$V_{u,2}$	123.6	37.7	103.6	31.6
$V_{x,1}$	308.8	94.1	319.8	97.5
$V_{x,2}$	385.8	117.6	381.4	116.2
V_1	790.4	240.9	813.1	247.8
V_2	405.1	123.5	395.2	120.5
W_1	383.6	116.9	404.4	123.3
W_2	733.3	223.5	714.0	217.6
	Angle, deg			
α_1	67.0		66.84	
β_1	36.38		37.75	
α_2	-17.77		-15.2	
β_2	-58.26		-57.71	

Figure 12. - Comparison of design velocity diagram at mean radius with that calculated from experimental results obtained at equivalent design speed and equivalent design specific work output. (All velocities in table correspond to turbine inlet conditions of U. S. standard sea-level air.)

"The aeronautical and space activities of the United States shall be conducted so as to contribute . . . to the expansion of human knowledge of phenomena in the atmosphere and space. The Administration shall provide for the widest practicable and appropriate dissemination of information concerning its activities and the results thereof."

—NATIONAL AERONAUTICS AND SPACE ACT OF 1958

NASA SCIENTIFIC AND TECHNICAL PUBLICATIONS

TECHNICAL REPORTS: Scientific and technical information considered important, complete, and a lasting contribution to existing knowledge.

TECHNICAL NOTES: Information less broad in scope but nevertheless of importance as a contribution to existing knowledge.

TECHNICAL MEMORANDUMS: Information receiving limited distribution because of preliminary data, security classification, or other reasons.

CONTRACTOR REPORTS: Scientific and technical information generated under a NASA contract or grant and considered an important contribution to existing knowledge.

TECHNICAL TRANSLATIONS: Information published in a foreign language considered to merit NASA distribution in English.

SPECIAL PUBLICATIONS: Information derived from or of value to NASA activities. Publications include conference proceedings, monographs, data compilations, handbooks, sourcebooks, and special bibliographies.

TECHNOLOGY UTILIZATION PUBLICATIONS: Information on technology used by NASA that may be of particular interest in commercial and other non-aerospace applications. Publications include Tech Briefs, Technology Utilization Reports and Notes, and Technology Surveys.

Details on the availability of these publications may be obtained from:

SCIENTIFIC AND TECHNICAL INFORMATION DIVISION

NATIONAL AERONAUTICS AND SPACE ADMINISTRATION

Washington, D.C. 20546